JOURNAL OF APPLIED ELECTROCHEMISTRY **27** (1997) 83–92

Electrochemical extraction of oxygen from air via hydroperoxide ion

E. BRILLAS, A. MAESTRO, M. MORATALLA

Departament de Química Física, Facultat de Química, Universitat de Barcelona, Martí i Franquès 1, 08028 Barcelona, Spain

J. CASADO

Departamento de Investigación, Carburos Metalicos SA, Pº Zona Franca 14-20, 08038 Barcelona, Spain

Received 24 October 1995

A novel electrochemical method for the extraction of pure oxygen from air is described. The system consists of an undivided cell with a nickel anode, a carbon–polytetrafluoroethylene (CP) air-fed cathode and a $KOH+HO_2^-$ solution as electrolyte. In such a Ni–CP cell, oxygen from the air is reduced in the cathode to form HO_2^- via a two-electron process, whereas anodic generation of oxygen gas can take place by the two-electron oxidation of HO_2^- and/or the four-electron oxidation of OH^- of the medium. Gas chromatography confirmed that the oxygen produced from cells operating up to $190\,mA\,cm^{-2}$ does not contain hydrogen, as expected if cathodic reduction of H_2O does not take place. The presence of HO_2^- causes a decrease in energy consumption of the cell, since it is easier to oxidize than OH^-. Ni–CP cells containing solutions with concentrations of OH^- to $2.4\,mol\,dm^{-3}$ and HO_2^- from 0.1 to $0.5\,mol\,dm^{-3}$ are stable at 25 °C for voltages to about 1.0 V. These cells work in a steady state in which the same number of moles of HO_2^- ions electrogenerated at the cathode are also anodically decomposed at the anode, without OH^- oxidation. In this state, the oxygen consumed in the cathode is anodically generated and extraction of oxygen from air occurs by a two-electron process. Energy consumptions between $1.710\,kW\,h\,kg^{-1}$ O_2 and $1.224\,kW\,h\,kg^{-1}$ O_2 are obtained for bielectronic stable cells operating at $100\,mA\,cm^{-2}$ and at temperatures between 25°C and 45 °C, which are significantly lower than those reported for previous electrochemical oxygen generators based on the anodic decomposition of OH^-.

1. Introduction

The most common method for electrochemical oxygen generation is by water electrolysis. The theoretical voltage for the electrolytic decomposition of water to hydrogen and oxygen gas is 1.23 V at 25°C, but the overvoltages, mainly at the anode, increase the working voltage to about 2.2 V at a current density (j) of $100\,mA\,cm^{-2}$ [1, 2]. The simultaneous production of evolved hydrogen as byproduct, along with high power requirements, are the main disadvantages for oxygen production from electrolysis of water. A more efficient electrolytic procedure consisting of the separation of oxygen from air via electrogeneration and electrooxidation of OH^- ions by a four-electron way has been reported by several authors [1–5]. In this method, air is injected to the cathode chamber of the cell where either a catalyst–polyethylene or a catalyst–polytetrafluoroethylene (PTFE) gas permeable electrode, usually a platinum black–PTFE cathode, is able to reduce oxygen to form OH^- ions by the following four-electron reaction:

$$O_2\text{ (from air)} + 2\,H_2O + 4\,e^- \longrightarrow 4\,OH^- \qquad (1)$$

The electrogenerated OH^- ions diffuse through a suitable membrane to the anode chamber where they are oxidized to oxygen in an oxygen-evolving anode via a four-electron process:

$$4\,OH^- \longrightarrow O_2(\text{pure}) + 2\,H_2O + 4\,e^- \qquad (2)$$

This procedure has allowed lower working voltages than those of electrolysis of water. Thus, Tseung and Jasem [2] found IR-corrected voltages of 1.3 V at 25 °C and 1.0 V at 40 °C at $100\,mA\,cm^{-2}$ in a two-compartment cell fed with air and which contained Pt–PTFE electrodes and $5.0\,mol\,dm^{-3}$ KOH as electrolyte. A minimum energy consumption of $438 \times 10^{-3}\,kW\,h\,dm^{-3}$ of oxygen at 40 °C which corresponds to $3.354\,kW\,h\,kg^{-1}$ O_2 was obtained.

The two-electron reduction of oxygen to hydrogen peroxide has been extensively studied in acidic and basic aqueous solutions using graphite electrodes and carbon–PTFE oxygen-fed electrodes [1, 6–14]. The highest current efficiencies for H_2O_2 generation (> 90%) have been reported for bipolar cells [7] and two-compartment H-cells [6, 10] containing OH^- concentrations higher or equal to $0.1\,mol\,dm^{-3}$. Since the pK_a for H_2O_2 is 11.64 at 25 °C, its conjugated base, the hydroperoxide ion (HO_2^-), is the species generated from oxygen electroreduction in such basic media, according to the process:

$$O_2(\text{from air}) + H_2O + 2\,e^- \longrightarrow HO_2^- + OH^- \quad (3)$$

The HO_2^- decays during its electrogeneration mainly due to its homogeneous chemical degradation to form O_2 and OH^- [1, 10, 13, 14] from the reaction:

$$2\,HO_2^- \longrightarrow O_2 + 2\,OH^- \quad (4)$$

which is favoured in strong alkaline media and is catalysed by metallic ions. Reaction 4 can also take place on the surface of metals, alloys and/or metal oxides (heterogeneous decomposition) in the cell.

Tseung and Jasem [2] have applied the self-degradation of HO_2^- to design an integrated electrochemical–chemical method for separation of oxygen from air in a three-chamber cell with 5.0 mol dm^{-3} KOH. In the cathode chamber, a floating graphite–PTFE cathode fed with air is used to reduce oxygen, producing HO_2^- from Reaction 3. The electrogenerated HO_2^- diffuses through a membrane to reach an intermediate chamber where it is chemically decomposed to oxygen on a nickel mesh coated with $NiCo_2O_4$, whereas in the anode chamber, OH^- is simultaneously oxidized to oxygen on a $NiCo_2O_4$–PTFE anode via Reaction 2. Energy consumptions of 2.645 kW h kg^{-1} O_2 at 25 °C and 2.058 kW h kg^{-1} O_2 at 40 °C were obtained for such a system working at 100 mA cm^{-2} with *IR*-free voltages of 1.34 V and 1.04 V, respectively.

Hydroperoxide ions electrogenerated by reduction of oxygen in basic medium could also be anodically oxidized to produce gaseous oxygen via the following two-electron process [13, 15]:

$$HO_2^- + OH^- \longrightarrow O_2(\text{pure}) + H_2O + 2\,e^- \quad (5)$$

However, electrochemical oxygen generators involving Reaction 5 have not been previously described in the literature.

The aim of the present work is to present a novel procedure for the electrochemical extraction of oxygen from ambient air by a two-electron process via electrogeneration and electrooxidation of HO_2^-. The electrochemical oxygen generator consists of an undivided cell with a nickel anode, a carbon–PTFE (CP) air-fed cathode and a KOH + HO_2^- solution as electrolyte. Nickel has been chosen as anode due to its poor catalytic activity for self-degradation of HO_2^- and its relatively low oxygen overvoltage. In the Ni–CP cell tested, oxygen from air is cathodically reduced to HO_2^- following Reaction 3. When HO_2^- content in the medium is low, oxygen is produced simultaneously by anodic oxidation of HO_2^- from Reaction 5 and of OH^- by Reaction 2, taking place a gradual accumulation of HO_2^- ions. A steady-state is reached in which only HO_2^- is oxidized at the anode and the extraction process $O_2(\text{air}) \rightarrow O_2(\text{pure})$ takes place by a two-electron process involving Reactions 3 and 5. The effect of OH^- and HO_2^- concentrations and of temperature on such a steady behaviour of the cell has been studied to establish its operative conditions as function of current density and voltage applied. Theoretical expressions to calculate the energy consumption of the system and to describe the amount of HO_2^- accumulated in it and of OH^- consumed from solution have also been derived.

2. Theoretical considerations

2.1. *Energy consumption*

Consider an electrochemical oxygen generator with a medium containing OH^- and HO_2^- ions, which operates at constant voltage V (in volts) and constant current I (in ampères) for a time t (in seconds). The electrical power (in kW h) supplied to this system can be written as follows:

$$\text{Power} = \frac{VIt}{3.6 \times 10^6} \quad (6)$$

If the oxygen generation in the anode can occur via the four-electron oxidation of OH^- (Equation 2) and/or the two-electron oxidation of HO_2^- (Equation 5), the moles of oxygen gas obtained will depend on the relative proportion between oxidized OH^- and HO_2^- ions. In such a case, the moles of electrons n_{anod} transferred to the anode per mole of oxygen produced will be between 4 and 2. Under steady-state conditions (at constant I and V), the n_{anod} value remains constant and hence, the oxygen weight obtained ($m(O_2)$ in kg) can be determined from the expression:

$$m(O_2) = \left(\frac{M(O_2)\,It}{n_{\text{anod}}F}\right) \times 10^{-3} \quad (7)$$

where $M(O_2)$ is the molecular weight of oxygen and F is the faraday constant. The theoretical energy consumption ϵ of the cell (in kW h kg^{-1} O_2) is then given from the ratio between Equation 6 and Equation 7, namely:

$$\epsilon = 0.838\, n_{\text{anod}} V \quad (8)$$

Equation 8 predicts that the energy consumption for an electrochemical oxygen generator under steady-state conditions is directly proportional to n_{anod} and to the applied voltage. When only OH^- is oxidized at the anode and $n_{\text{anod}} = 4$, this equation is reduced to the following expression:

$$\epsilon = 3.355\, V \quad (9)$$

Note that setting $V = 1$ V in Equation 9, $\epsilon =$ 3.355 kW h kg^{-1} O_2, as experimentally reported for a cell fed with air working at 100 mA cm^{-2} and at 40 °C [2]. This confirms the applicability of Equation 9 to systems without HO_2^- present in the medium. By contrast, if only HO_2^- is anodically decomposed in the cell and $n_{\text{anod}} = 2$, Equation 8 can be expressed as follows:

$$\epsilon = 1.677\, V \quad (10)$$

Comparison of Equations 9 and 10 indicates that an electrochemical oxygen generator with $n_{\text{anod}} = 4$ has two times the energy consumption than another with $n_{\text{anod}} = 2$ operating at the same voltage under steady-state conditions, although both cells are expected to work at different current densities. In practice, it seems better to compare the energy consumptions for different systems from Equation 8 by applying the same j, then determining n_{anod} and V.

2.2. *Accumulation of HO_2^-*

Consider an electrochemical oxygen generator containing a basic solution and a cathode fed with oxygen from air which only produces HO_2^- from Equation 3. When the system works at constant current I for a time t, the number of moles of hydroperoxide ions ($n(HO_2^-)$) obtained from the two-electron reduction of oxygen is given by the equation:

$$n(HO_2^-) = \frac{It}{2F} \qquad (11)$$

If the self-decomposition of electrogenerated HO_2^- ions is negligible, they can be accumulated in solution depending on n_{anod} value. For $n_{\text{anod}} = 2$ all these ions are anodically decomposed to oxygen, for $n_{\text{anod}} = 4$ they remain in the medium since only OH^- is oxidized at the anode. However, when $2 < n_{\text{anod}} < 4$, a part of HO_2^- is oxidized and then, the moles of the remainder ions accumulated in the medium (i.e., moles of HO_2^- generated by Reaction 3 less the moles of HO_2^- oxidized by Reaction 5) is equal to the moles of OH^- consumed from solution (i.e., moles of OH^- consumed by Reactions 2 and 5 less the moles of OH^- produced by Reaction 3). These amounts for both species can be determined assuming that the cell works under steady-state conditions for a time large enough to produce 1 mol of O_2 at constant n_{anod}. If x mol O_2 proceed from the four-electron oxidation of OH^- and the remaining $(1 - x)$ moles of O_2 are obtained from the two-electron oxidation of HO_2^-, the overall n_{anod} electrons transferred to the anode must be equal to the sum of $4x$ electrons from Reaction 2 plus $2(1 - x)$ electrons from Reaction 5. In other words,

$$n_{\text{anod}} = 4x + 2(1 - x) \qquad (12)$$

Solving Equation 12, one obtains $x = (n_{\text{anod}}/2) - 1$. Taking also into account that the fraction of current used to oxidize HO_2^- is $2(1 - x)/n_{\text{anod}}$, the fraction of these ions remaining in solution is:

$$1 - \frac{2(1-x)}{n_{\text{anod}}} = \frac{2n_{\text{anod}} - 4}{n_{\text{anod}}} \qquad (13)$$

By multiplying the second member of Equation 13 by the total moles of HO_2^- generated in time t given by Equation 11, the moles of HO_2^- accumulated in the medium and of OH^- consumed from solution can be calculated in the form:

$$n(HO_2^-)\text{ accumulated} = n(OH^-)\text{ consumed} = \frac{I}{F}\frac{(n_{\text{anod}} - 2)\,t}{n_{\text{anod}}} \qquad (14)$$

Equation 14 can be applied when n_{anod} has a constant value. If this parameter varies with electrolysis time and $(n_{\text{anod}} - 2)/n_{\text{anod}}$ is given as an analytical function of time, the third member of Equation 14 can be applied to an infinitesimal time dt and integrated for the total process to obtain

$$n(HO_2^-)\text{ accumulated} = n(OH^-)\text{ consumed} = \frac{I}{F}\int_0^t \frac{(n_{\text{anod}} - 2)}{n_{\text{anod}}}\,dt \qquad (15)$$

Equation 15 provides a general theoretical expression to calculate the moles of HO_2^- accumulated and of OH^- consumed in the electrochemical oxygen generator as a function of the overall electrolysis time t when the change in n_{anod} value during the experiment is known and no significant self-degradation of HO_2^- takes place.

3. Experimental details

3.1. *Reagents*

A concentrated hydrogen peroxide solution of 33% w/w from Probus, analytical grade, was used to obtain standardized HO_2^- solutions in different KOH media. Potassium hydroxide, potassium permanganate and other chemicals (all AR) employed were Merck. Solutions were prepared with water obtained from a Millipore Milli-Q system. The conductivity of the water used was always lower than $6 \times 10^{-8}\,\Omega^{-1}\,\text{cm}^{-1}$.

3.2. *Instruments*

Electrolyses were performed with a Thurlby–Thandar PL330 power source. Linear sweep voltammetric measurements were carried out with a PAR 273A potentiostat–galvanostat connected to a PS-486DX microcomputer and controlled through a PAR M270 program. The content of hydrogen in oxygen gas evolved from cell was determined by gas chromatography (GC) using a Hewlett Packard 5890 series II gas chromatograph with a thermic conductivity detector and fitted with a 60/80 Carboxen 1000 column at 35 °C. GC data were collected on a HP 3395 integrator.

3.3. *Electrochemical cell*

A scheme of the Ni–CP cell used to produce oxygen from air is shown in Fig. 1. It was a one-compartment glass cylindric cell with an upper outlet tube to collect the evolved gases and a double-wall to permit circulation of water for controlling the system temperature. The nickel anode and the carbon-PTFE cathode were placed at the bottom of two cylindric holders of polypropylene and introduced face-to-face into it. The electrode distance was adjusted by regulating the separation between the extremes of both holders. In most of experiments, an interelectrode gap of

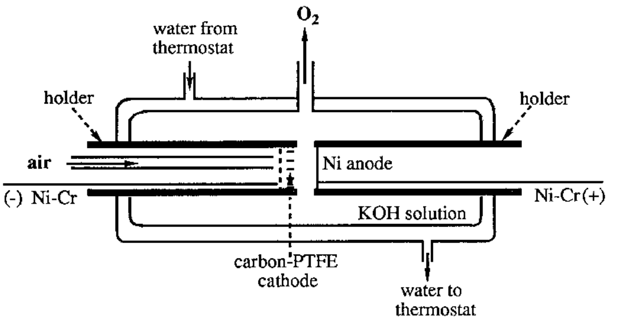

Fig. 1. Schematic representation of the Ni–CP cell used for the bielectronic electrochemical production of oxygen from air. The carbon–PTFE cathode was fed with an air flow of 140 ml min^{-1}.

5 mm was chosen. A pump was used to feed an air flow of 140 ml min^{-1} to the cathode through a glass tube inside its holder, the top of which was open to the atmosphere. Nichrome (Ni–Cr) wires were used as electrical contacts.

Once assembled, the cell was filled with 50 ml solution through its upper tube. In galvanostatic experiments, a gas burette was attached to the top of this tube to measure the oxygen generated. The carbon–PTFE cathode fed with an air flow of 140 ml min^{-1} was steady during all electrolyses. No gas bubbles were observed under the experimental conditions tested, indicating that air flowing over its inner face did not pass into the solution, the major part being rejected to the atmosphere through the top of the holder. This was confirmed by the fact that no gas was collected in the gas burette when the cell was in open circuit. During electrolyses, only a fraction of the oxygen diffused through the cathode to reach its outer face, where it was reduced to HO_2^- following Equation 3.

3.4. *Preparation of electrodes*

A nickel disc of 99.997% purity and 15 mm diameter × 0.10 mm thickness supplied by Johnson Matthey was used as anode.

The oxygen-diffusion cathode was composed of a reactive carbon–PTFE layer stacked onto a nickel screen of 200 mesh and 0.11 mm thick as current collector. The outer face of the electrode was the carbon–PTFE layer and its inner face was the nickel screen which was in contact with the Ni–Cr wire. This layer was prepared with carbon black Printex L (surface area 136 $\mathrm{m}^2\,\mathrm{g}^{-1}$) supplied by Degussa, which was bonded with 25% w/w PTFE dispersion of type 30-N from Du Pont de Nemours by means of the following method [16]: the carbon black was suspended in water with 3% w/w *n*-butanol as dispersant. PTFE dispersion was added and mixed. The resulting suspension was heated at 240 °C to remove water, *n*-butanol and all dispersants contained in PTFE. The obtained carbon–PTFE cake was milled into fine powder. A powder mass of 45 mg was cold-pressed onto a nickel screen of 15 mm diameter, and hot-pressed between two laminated steel cylinders at a pressure of 160 kg cm^{-2} and at 390 °C for 30 min. The carbon–PTFE cathode thus prepared was 0.40 mm thick.

Once the electrodes were mounted in the corresponding holders, the apparent area of the anode and the cathode in contact with solution was 0.785 cm^2.

3.5. *Electrochemical experiments*

Solutions of KOH concentration between 0.8 mol dm^{-3} and 10.4 mol dm^{-3} were studied in electrolysis experiments. The effect of hydroperoxide ions on the behaviour of the cell was investigated in KOH solutions containing HO_2^- concentrations to 0.5 mol dm^{-3}. At higher HO_2^- concentrations, the fast self-decomposition of this species to O_2 and OH^- prevented from achieving operative steady-state conditions. The temperature was usually maintained at 25°C, although several electrolyses at 35°C and 45 °C were also performed to study the effect of solution temperature upon the efficiency of the cell. Prior to being used, the cathode was activated *in situ* by applying a voltage of 1.60–1.80 V for a minimum of 5 min.

Linear sweep voltammograms for the oxidation of OH^- and/or HO_2^- to form O_2 on the nickel anode, as well as for reduction of O_2 to yield HO_2^- in the carbon–PTFE cathode, were recorded in 0.8 mol dm^{-3} KOH at a scan rate of 5 mV s^{-1} and at 25 °C. A SSCE (NaCl-saturated calomel electrode) was used as reference electrode, which was introduced into the cell through its upper tube to be in contact with the solution.

3.6. *Analysis procedure*

The HO_2^- concentration present in the medium before and during electrolyses was obtained by standard titration of 1 ml aliquots with potassium permanganate. The change in OH^- concentration was determined by titration of 2 ml aliquots with standardized 0.1 mol dm^{-3} HCl. To know the content of hydrogen gas in the oxygen produced, gases evolved in several galvanostatic experiments were periodically collected in inverted test tubes, initially filled with water. A volume of 300 μl of samples was directly injected to gas chromatograph and detection of hydrogen was performed using a nitrogen flow of 50 ml min^{-1} as carrier gas. Under these conditions, a well-defined sharp peak of hydrogen was found for a standard sample of air with 0.96% v/v H_2.

3.7. *Determination of n_{anod} in galvanostatic experiments*

The n_{anod} value for a cell working at constant I during a given t was determined experimentally from the volume of oxygen $V(O_2)$ collected in the gas burette. This volume (in dm^3) was measured at ambient temperature (T_{amb}) between 293 K and 297 K, at an average atmospheric pressure (P_{atm}) of 0.984 atm. Having

n_{anod} a constant value during this electrolysis, the number of moles of O_2 ($n(O_2)$) produced by the cell can be calculated as follows:

$$n(O_2) = \frac{It}{n_{\text{anod}}F} \tag{16}$$

Assuming that oxygen behaves as an ideal gas, these moles of oxygen can also be calculated from its state equation. Combining both expressions, the n_{anod} value can be obtained by the following equation:

$$n_{\text{anod}} = \frac{8.65 \times 10^{-7}\, T_{\text{amb}}It}{V(O_2)} \tag{17}$$

4. Results and discussion

4.1. *Behaviour of the Ni–CP cell containing a KOH solution*

The oxygen from air injected to the cathode of a Ni–CP cell containing a KOH solution is expected to be reduced to form HO_2^- (Reaction 3) when the applied voltage is small enough to avoid other cathodic reactions, such as reduction of H_2O to H_2 and OH^- and/or HO_2^- to OH^- [12, 13]. However, oxygen can be produced at the nickel anode by the simultaneous oxidation of OH^- (Reaction 2) and electrogenerated HO_2^- (Reaction 5). At the beginning of the electrolysis, the HO_2^- content in solution is negligible and only decomposition of OH^- occurs with $n_{\text{anod}} = 4$, whereas as long as HO_2^- is competitively oxidized by increasing electrolysis time, a variation of n_{anod} value between 4 and 2 is expected.

To confirm whether the cell behaves as stated above, several electrolyses with 50 ml of 2.4 mol dm^{-3} KOH as initial solution were performed at a constant current density of 100 mA cm^{-2} for 10 h. In these experiments, the electrode distance was adjusted to 5 mm. The volume of oxygen produced and the applied voltage were measured every 20 min. The change in HO_2^- and OH^- concentrations were determined in different runs to avoid large losses of solution volume. Under these conditions, no hydrogen gas was detected by GC in the evolved oxygen, thus indicating that cathodic reduction of H_2O to H_2 and OH^- does not occur.

Typical variations of n_{anod} and ϵ found with electrolysis time are given in Fig. 2. A progressive decrease from $n_{\text{anod}} = 4$ at the beginning of the electrolysis to $n_{\text{anod}} = 2.16$ after 10 h of it can be observed in Fig. 2(a), as expected if the system evolves slowly to a steady-state with $n_{\text{anod}} = 2$. This indicates a gradual increase in the electrodecomposition rate of HO_2^-, associated with the presence of a higher content of this species in the medium, as will be discussed below from results of Fig. 3. In addition, the working voltage also decays gradually from an initial value of 1.29 V to a final value of 1.08 V. The simultaneous decrease of n_{anod} and applied voltage explains the progressive decay in ϵ during electrolysis, as shown in Fig. 2(b). This trend of ϵ indicates that cells with KOH + HO_2^- solutions have lower energy consumptions as HO_2^- concentration increases.

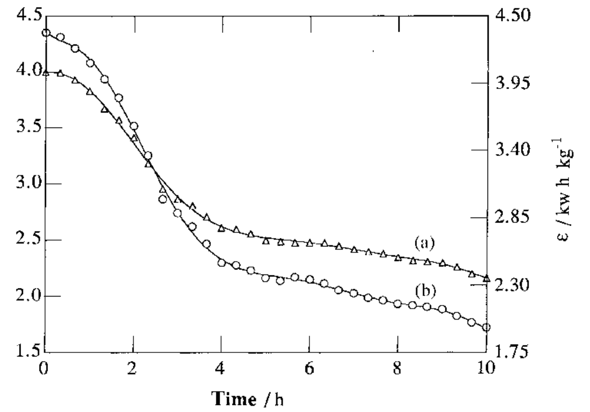

Fig. 2. (a) Change of the moles of electrons transferred to the anode per mole of oxygen produced (n_{anod}) calculated from Equation 17 with electrolysis time for a Ni–CP cell with 2.4 mol dm^{-3} KOH operating at 100 mA cm^{-2} for 10 h at 25 °C. (b) Variation of energy consumption ϵ of the cell determined from Equation 8 with electrolysis time.

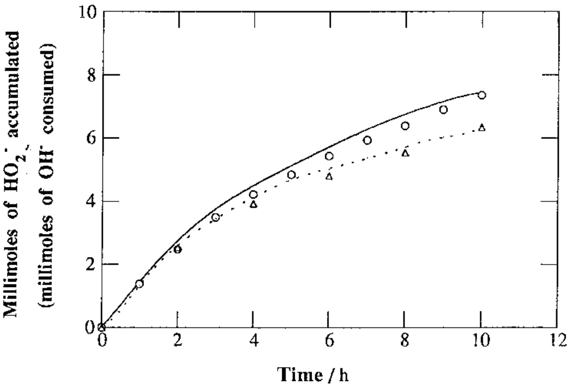

Fig. 3. (○) Millimoles of HO_2^- accumulated in a Ni–CP cell for the same electrolysis as in Fig. 2. The solid line corresponds to the theoretically expected curve from Equation 15 using the n_{anod} values given in Fig. 2(a). (△) Millimoles of OH^- consumed from solution for a different run of the cell. The dashed line is the theoretical curve obtained from Equation 15.

The possible self-degradation of HO_2^- was studied by filling up the cell with different KOH media containing HO_2^- concentrations of 0.1 and 0.5 mol dm^{-3} during 10 h without passing current, conditions under which this species can only be destroyed by Reaction 4. The percentage of remaining HO_2^- was found to be 97–99% in 0.8 mol dm^{-3} KOH, 92–94% in 2.4 mol dm^{-3} KOH and 78–82% in 5.2 mol dm^{-3} KOH, for both HO_2^- concentrations considered. These results confirm a faster chemical decomposition rate for HO_2^- as long as OH^- concentration increases. According to this, Equation 15 which assumes no self-degradation of this species can be applied to explain its accumulation in Ni–CP cells with KOH concentrations lower or equal to 2.4 mol dm^{-3}, that is, when the rate of Reaction 4 is so slow that it can be assumed to be negligible.

Figure 3 shows the gradual increase found experimentally for the millimoles of HO_2^- accumulated in solution during the same electrolysis as in Fig. 2. The solid line in Fig. 3 corresponds to the theoretical curve calculated from Equation 15 by fitting the experimental function $(n_{\text{anod}} - 2)/n_{\text{anod}}$ obtained from values of Fig. 2(a) against electrolysis time to an eight-order polynomial with a regression coefficient $r = 0.9992$. The progressive increase in the OH^- consumed from solution is also presented in Fig. 3 for another run of the cell, along with the corresponding theoretical line (dashed curve) calculated from Equation 15, also considering an eight-order polynomial function between $(n_{\text{anod}} - 2)/n_{\text{anod}}$ and t with $r = 0.9990$. As can be seen, the experimental change of HO_2^- accumulated and OH^- consumed with electrolysis time is well-described by Equation 15 for each electrolysis, although slightly different experimental points and theoretical curves were obtained for different runs. The shape of these curves indicates a progressive decrease in accumulation rate of HO_2^- as electrolysis time increases, due to the gradual increase of its anodic decomposition rate, in agreement with the parallel decrease found for n_{anod} (see Fig. 2(a)). The fact that the theoretical curve obtained from Equation 15 can describe the change in HO_2^- during electrolysis, suggests that most of these ions are either anodically oxidized from Reaction 5 or remain in solution. Data reported in Fig. 3 show that after 10 h of electrolysis at 100 mA cm^{-2}, an average value of 6.9 ± 0.5 mmol HO_2^- or OH^- were either accumulated or consumed in the cell. Since in each electrolysis 18.7 mmol HO_2^- were generated considering that only Reaction 3 occurs in the cathode, it can be concluded that $63 \pm 3\%$ of this species is decomposed to oxygen gas.

4.2. *Addition of H_2O_2 to the cell*

As Ni–CP cells initially containing a KOH solution evolved slowly with electrolysis time to a steady-state with accumulation of HO_2^-, the behaviour of cells with KOH + HO_2^- solutions was studied by determining the steady current densities reached when constant voltages from 0.1 to 1.5 V were applied. Electrolyses were performed for electrode distances between 5 mm and 14 mm and for KOH concentrations between 0.8 mol dm^{-3} and 10.4 mol dm^{-3}, both in the presence and in the absence of added H_2O_2. For HO_2^- concentrations higher than 0.8 mol dm^{-3}, the solutions released large amounts of oxygen due to its fast chemical degradation. To avoid this process as much as possible, the maximum HO_2^- concentration tested in experiments was limited to 0.5 mol dm^{-3}.

In all media and for a given voltage, the steady current density increased by shortening the electrode distance, as expected by the simultaneous decay in ohmic drop between electrodes. However, no steady j values could be measured for electrode distances shorter than 5 mm by perturbations of the oxygen bubbles released from the anode. For this reason, an optimum interelectrode gap of 5 mm was used to study the behaviour of Ni–CP cells.

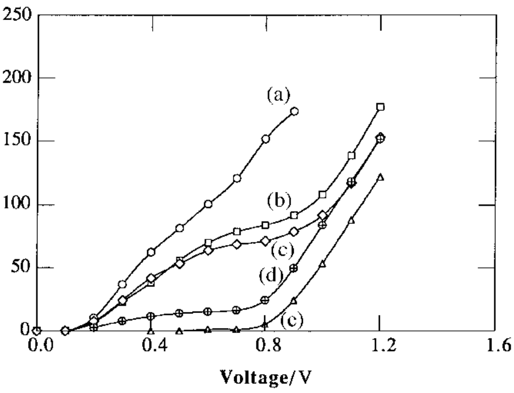

Fig. 4. Current density-voltage plots for a Ni–CP cell containing 5.6 mol dm^{-3} KOH with HO_2^- concentrations of: (a) 0.475, (b) 0.292, (c) 0.200, (d) 0.042 mol dm^{-3}. Curve (e) was obtained without addition of H_2O_2 to the medium. Temperature 25°C.

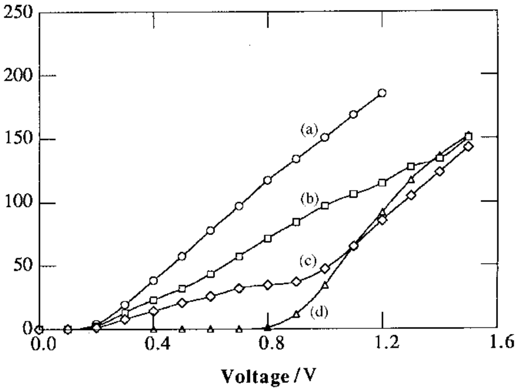

Fig. 5. Current density–voltage plots for a Ni–CP cell with 2.4 mol dm^{-3} KOH and HO_2^- concentrations of: (a) 0.510, (b) 0.204, (c) 0.085 mol dm^{-3}. Curve (d) was determined without addition of H_2O_2 to the medium. Temperature 25°C.

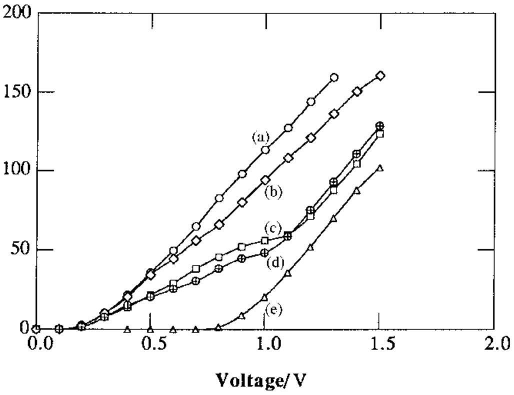

Fig. 6. Current density–voltage relationships for a Ni–CP cell with 0.8 mol dm^{-3} KOH and HO_2^- concentrations of: (a) 0.450, (b) 0.202, (c) 0.115, (d) 0.066 mol dm^{-3}. Curve (e) was obtained without addition of H_2O_2 to the medium. Temperature 25°C.

Figures 4, 5 and 6 show the steady j/V relationships obtained for 5.6, 2.4 and 0.8 mol dm^{-3} KOH solutions, respectively, without HO_2^- and with different concentrations of this species. Comparison of curves measured in the absence of this ion allows us to conclude that at a given voltage the corresponding j value for 2.4 mol dm^{-3} KOH (Fig. 5(d)) is much higher than for 0.8 mol dm^{-3} KOH (Fig. 6(e)) and only slightly lower than for 5.6 mol dm^{-3} KOH (Fig. 4(e)). Similar j/V plots to those given in Figs 4(e) and 5(d) were also found for 6.3, 8.8 and 10.4 mol dm^{-3} KOH. This behaviour can be ascribed to a gradual increase in conductivity of KOH solution from 0.8 to 2.4 mol dm^{-3}, which causes a progressive decrease of ohmic drop between electrodes. However, for KOH concentrations higher than 2.4 mol dm^{-3}, the *IR* product between electrodes reaches a minimum value, having little influence upon the cell voltage.

In all KOH media and in the presence of HO_2^- (see Figs 4–6), the current rises at a voltage of about 0.2 V, whereas in the absence of this species a minimum voltage of about 0.9 V must be applied to begin to produce oxygen in the anode. This decrease of almost 0.7 V in working voltage can be ascribed to the anodic oxidation of HO_2^- instead of that of OH^-. The *j*/*V* plots obtained in all KOH solutions with the lowest HO_2^- concentrations showed a plateau, which can be associated with a diffusive control in the anodic oxidation process of HO_2^-, since at higher potentials, the simultaneous oxidation of OH^- caused a notable increase in current density. For the highest HO_2^- concentrations, the oxidation rate of this ion increased gradually with cell voltage and *j*/*V* plots did not display any plateau (see Figs 4(a), 5(a) and 6(a)).

The above results allow us to establish that cells containing KOH + HO_2^- solutions can work to about 1.0 V producing oxygen from the two-electron anodic decomposition of HO_2^-, with practically no oxidation of OH^-. Under these conditions, operative current densities between 100 mA cm^{-2} and 150 mA cm^{-2} can be easily reached for HO_2^- concentrations higher than 0.2 mol dm^{-3}, as can be deduced from results shown in Figs 4–6.

4.3. *Study of the anodic and cathodic reactions by linear sweep voltammetry*

The fact that HO_2^- is oxidized at less positive potentials than OH^- was confirmed by linear sweep voltammetry. Figure 7 shows different voltammograms recorded for the anodic oxidation of both ions in a cell containing a 0.8 mol dm^{-3} KOH solution. The solid line corresponds to the tetraelectronic decomposition of OH^- on nickel to O_2 following Reaction 2, which begins at 0.50 V vs SSCE. In the presence of HO_2^-, the oxidation curves (Fig. 7(a)–(c)) were shifted at less anodic potentials due to the bielectronic anodic decomposition of this species to oxygen from Reaction 5. Figure 7(a)–(c) shows that HO_2^- is oxidized on nickel from −0.13 V vs SSCE, independently of its concentration. In addition, a plateau at potentials between 0.2 V and 0.6 V vs SSCE can be observed from the voltammogram recorded at 0.105 mol dm^{-3} HO_2^- (Fig. 7(c)), indicating that the oxidation process of this ion is limited by its diffusive transport to the anode limits. This kind of control was not found for HO_2^- concentrations higher than 0.2 mol dm^{-3} (Fig. 7(a)–(b)), due to the gradual increase in its oxidation rate and overlapping with anodic decomposition of OH^-.

Voltammograms obtained for the two-electron cathodic reduction of oxygen from air to HO_2^- by Reaction 3 in the above Ni–CP cell are shown in Fig. 8, without HO_2^- (solid curve) and with different concentrations of this species. In all media, the reduction of oxygen on the carbon–PTFE cathode was found to rise at −0.32 V vs SSCE and its rate increased progressively as long as potentials shifted to more negative values.

The above results can explain that addition of H_2O_2 to a KOH solution causes a strong decay of the initial operative voltage of the cell, as Figs 4–6 show. This is mainly due to the easier oxidation ability of HO_2^- on nickel, which starts to be decomposed at a potential 0.63 V less anodic than for OH^- (see Fig. 7). Voltammetric results also corroborate that the plateau observed for *j*/*V* plots of Figs 4–6 in KOH + HO_2^- media is due to the diffusive control of its decomposition at the nickel anode (see Fig. 7(a)–(c)), since no effect upon the reduction process of oxygen at the cathode was observed in such conditions (see Fig. 8).

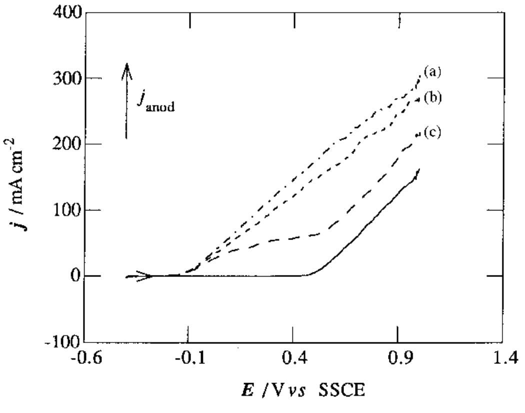

Fig. 7. Linear sweep voltammograms recorded for the oxidation of HO_2^- on the nickel anode of a Ni–CP cell containing a 0.8 mol dm^{-3} KOH solution with HO_2^- concentrations of: (a) 0.468, (b) 0.230, (c) 0.105 mol dm^{-3}. The solid curve corresponds to the tetraelectronic oxidation of OH^- to O_2 and was obtained without addition of H_2O_2 to the medium. Initial potential −0.4 V and final potential 1.0 V. Scan rate 5 mV s^{-1}, temperature 25 °C.

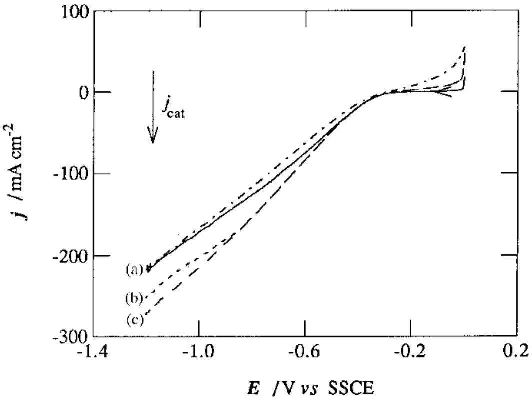

Fig. 8. Linear sweep voltammograms obtained for the reduction of O_2 to HO_2^- in the carbon–PTFE air-fed cathode of a Ni–CP cell with 0.8 mol dm^{-3} KOH and HO_2^- concentrations of: (a) 0.468, (b) 0.230, (c) 0.105 mol dm^{-3}. The solid line was recorded without addition of H_2O_2 to the medium. Initial potential 0 V and final potential −1.2 V. Scan rate 5 mV s^{-1}, temperature 25 °C.

4.4. *Stability of Ni–CP cells containing KOH + HO_2^- solutions*

Cells with different KOH + HO_2^- media were electrolysed under several experimental conditions to study their stability. A cell was considered stable when composition of its medium remained unchanged working at constant *j* and *V*. A first series of experiments were performed with standardized HO_2^- concentrations from 0.1 to 0.5 mol dm^{-3} in 5.6, 2.4 and 0.8 mol dm^{-3} KOH, operating at 0.70 V and at 25 °C, conditions under which only the anodic oxidation of HO_2^- takes place (see Figs 4–6). Cells containing 5.6 mol dm^{-3} KOH solutions were unsteady, being observed a gradual decrease of *j* and HO_2^- content with electrolysis time. This same behaviour was found for cells with 2.4 mol dm^{-3} KOH and HO_2^- concentrations higher than 0.3 mol dm^{-3}. Since the decrease in HO_2^- content can be due to its self-degradation, electrolyses with 2.4 mol dm^{-3} KOH were effected again in the presence of 1.5 mmol dm^{-3} urea as stabilizer.

The current densities determined for stable cells working at 0.70 V and containing 2.4 and 0.8 mol dm^{-3} KOH are presented in Figs 9 and 10, respectively. The concentration of HO_2^- and OH^- remained constant during all experiments. A progressive increase in *j* with increasing HO_2^- concentration can be observed for each KOH solution, although higher current densities were obtained for 2.4 mol dm^{-3} KOH (Fig. 9) than for 0.8 mol dm^{-3} KOH (Fig. 10). The stability in 0.8 mol dm^{-3} KOH was confirmed by electrolysing a solution with 0.440 mol dm^{-3} HO_2^- at 0.70 V for 22.5 h. A steady current density of 56 ± 2 mA cm^{-2} was found during electrolysis and the final HO_2^- concentration was 0.422 mol dm^{-3}.

A second series of experiments attempted to confirm if simultaneous anodic decomposition of OH^- occurs for working voltages higher than about 1.0 V. Figure 11 shows the variation of volume of oxygen released with electrolysis time when 38, 100 and 190 mA cm^{-2} were applied to a cell with 2.4 mol dm^{-3} KOH and 0.182 mol dm^{-3} HO_2^-. GC analysis corroborated the absence of hydrogen gas in oxygen produced during these electrolyses, even operating at 190 mA cm^{-2}. Stationary voltages of 0.70 ± 0.02 V and 1.03 ± 0.02 V were measured for 38 and 100 mA cm^{-2}, respectively, whereas at 190 mA cm^{-2} the working voltage decreased gradually from an initial value of 1.61 to 1.46 V after 9 h of electrolysis. Straight lines in Fig. 11 correspond to the volumes of oxygen calculated from Equation 17 taking $n_{anod} = 2$. As can be seen, theoretical lines of Fig. 11(b) and (c) agree with the respective experimental points obtained for 100 and 38 mA cm^{-2}. In both cases, the composition of medium did not vary and the cell was stable. However, the theoretical line of Fig. 11(a) does not fit the volumes of oxygen collected at 190 mA cm^{-2}. A progressive decrease from 2.38 to 2.05 for n_{anod} value calculated by Equation 17 was found during this electrolysis, whereas 4.65 mmol HO_2^- were accumulated in solution and an equivalent amount of OH^- was consumed. Then, at 190 mA cm^{-2} and at

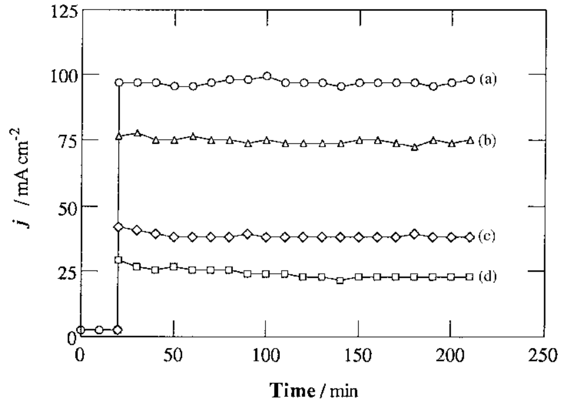

Fig. 9. Change of current intensity of a Ni–CP cell containing 2.4 mol dm^{-3} KOH with electrolysis time. The cell operated at a constant voltage of 0.70 V and after 20 min from the beginning of electrolysis, a HO_2^- concentration of: (a) 0.518, (b) 0.275, (c) 0.181, (d) 0.095 mol dm^{-3} was added to the medium, which remained constant during experiments. In the case (a) the solution contained 1.5 mmol dm^{-3} urea. Temperature 25°C.

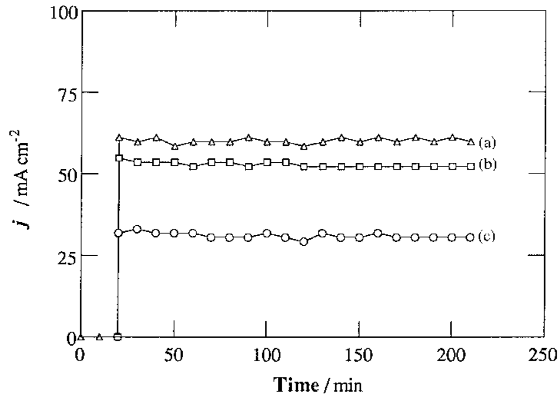

Fig. 10. Dependence of current density on electrolysis time for a Ni–CP cell containing 0.8 mol dm^{-3} KOH and operating at a constant voltage of 0.70 V. After 20 min from the beginning of electrolysis, a HO_2^- concentration of: (a) 0.510, (b) 0.201, (c) 0.113 mol dm^{-3} was added to the medium. In all cases, no change in HO_2^- concentration was detected during electrolysis. Temperature 25°C.

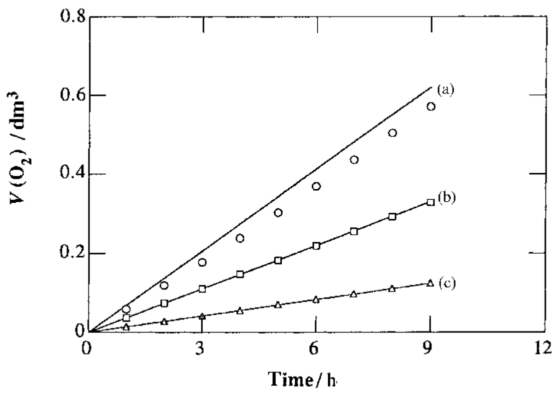

Fig. 11. Variation of volume of oxygen produced by a Ni–CP cell containing 2.4 mol dm^{-3} KOH and 0.182 mol dm^{-3} HO_2^- with electrolysis time by applying a constant current density of : (a) 190, (b) 100, (c) 38 mA cm^{-2}. The respective solid lines correspond to the theoretical volumes of oxygen calculated from Equation 17 which are expected to be generated by a cell with $n_{anod} = 2$ under the same experimental conditions. In cases (b) and (c), HO_2^- concentration remained constant, whereas in the case (a) it gradually increased to 0.275 mol dm^{-3} after 9 h of electrolysis. Temperature 25 °C.

Table 1. Values of n_{anod} and energy consumptions determined for stable Ni–CP cells fed with an air flow of 140 ml min^{-1} and operating at constant current density under different experimental conditions for 3 h

[KOH] /mol dm^{-3}	*[HO_2^-]* /mol dm^{-3}	*Solution temperature*/°C	*j*/mA cm^{-2}	*Voltage*/V	n_{anod}*	$\epsilon^{\dagger}$/kW h kg^{-1} O_2
0.8	0.121	25	38	0.89	1.99	1.492
	0.216	25	38	0.57	2.01	0.955
	0.381	25	38	0.52	1.96	0.872
		25	100	1.02	2.05	1.710
		35	100	0.90	2.00	1.509
		45	100	0.86	1.95	1.442
	0.498‡	25	100	1.01	1.98	1.693
2.4	0.124	25	38	0.76	1.97	1.275
	0.185	25	38	0.68	1.99	1.140
	0.246	25	38	0.60	1.99	1.006
	0.185	25	100	1.02	2.00	1.710
		35	100	0.90	1.97	1.509
		45	100	0.82	1.97	1.375
	0.266	25	100	0.98	2.03	1.643
		35	100	0.85	1.96	1.425
		45	100	0.77	1.98	1.291
	0.462‡§	25	100	0.73	1.98	1.224

* Moles of electrons transferred to the anode per mole of oxygen gas produced by the cell calculated from Equation 17.

† Energy consumption determined from Equation 8 considering $n_{anod} = 2$.

‡ Cells were unstable at 35 °C and at 45 °C.

§ Solution contained 1.5 mmol dm^{-3} urea.

voltages higher than 1.0 V the cell was unsteady and a part of electrogenerated HO_2^- and OH^- were oxidized at the anode.

4.5. *Ni–CP cells operating at constant current density under steady-state conditions*

The above findings indicate that for given *j* and *V* values the energy consumption of stable Ni–CP cells must depend on the solution tested and on its temperature. To know their operative conditions, cells with different $KOH + HO_2^-$ solutions were electrolysed at 38 or 100 mA cm^{-2} and different temperatures for 3 h. Table 1 summarizes the media used, the solution temperature, the current density applied, the cell voltage and the n_{anod} value determined from Equation 17, and for all experiments tested. Since no change in composition of media was found after all electrolyses and the obtained n_{anod} values were always close to 2, energy consumptions given in the last column of Table 1 have been calculated from Equation 8 considering $n_{anod} = 2$. It is then apparent that all reported cells were stable and operated in a steady-state in which the same moles of HO_2^- generated in the carbon–PTFE cathode are also oxidized at the nickel anode, making it possible that the same amount of oxygen consumed at the cathode is anodically produced.

Results of Table 1 indicate that at given *j* and temperature the voltage and energy consumption of the cell decreases gradually by increasing HO_2^- concentration for each KOH solution, in agreement with results shown in Figs 5 and 6. In addition, an increase of temperature in a given medium at constant *j* causes a decrease in ϵ due to the simultaneous fall of the applied voltage, according to the expected *IR* decay between electrodes. Cells containing HO_2^- concentrations higher than 0.4 mol dm^{-3} were unsteady at 35 °C and at 45 °C, and showed a continuous loss of HO_2^- content by self-degradation.

Bielectronic Ni–CP cells working under steady-state conditions yield lower ϵ values (see Table 1) than those given in the literature for previous electrochemical oxygen generators. Although the lowest reported energy consumption for such devices at 100 mA cm^{-2} is 2.058 kW h kg^{-1} O_2 at 40 °C [2], the lowest ϵ obtained for a stable Ni–CP cell at 100 mA cm^{-2} is 1.224 kW h kg^{-1} O_2 at 25 °C. This is achieved using a 2.4 mol dm^{-3} KOH solution with 0.462 mol dm^{-3} HO_2^- and 1.5 mmol dm^{-3} urea, as shown in Table 1. At lower current densities, energy consumptions lower than 1 kW h kg^{-1} O_2 can be easily obtained.

5. Conclusions

In a Ni–CP cell containing a KOH solution and fed with air, HO_2^- is generated at the cathode by the two-electron reduction of oxygen from air following Reaction 3 and is anodically decomposed to yield oxygen gas via the two-electron Reaction 5. Under all experimental conditions tested, no cathodic reduction of H_2O to H_2 and OH^- occurs, as tested by GC. When no HO_2^- is present in solution, oxygen gas is produced at the nickel anode by the four-electron oxidation of OH^- from Reaction 2. As long as HO_2^- is electrogenerated, a part of this species is oxidized and the remaining one is accumulated in the medium due to the simultaneous oxidation of OH^-. Accumulation of HO_2^- and simultaneous consumption of OH^- are well-described by Equation 15 when self-degradation of HO_2^- is negligible. The anodic oxidation rate of HO_2^- increases with increasing its content in solution, causing a progressive decay in energy consumption of the cell.

By increasing HO_2^- concentration to $0.5\,\mathrm{mol\,dm^{-3}}$ in KOH solutions, Ni–CP cells showed a gradual increase in their steady current densities at voltages lower than 1.5 V. The initial operative voltage for cells with $KOH + HO_2^-$ solutions decreased almost 0.7 V with respect to cells only containing KOH due to the easier oxidation of HO_2^- than that of OH^- at the nickel anode, as confirmed by linear sweep voltammetry. Several Ni–CP cells with OH^- concentrations to $2.4\,\mathrm{mol\,dm^{-3}}$ and HO_2^- concentrations from 0.1 to $0.5\,\mathrm{mol\,dm^{-3}}$ were stable by applying voltages to about 1.0 V. These cells work in a steady-state with $n_{\mathrm{anod}} = 2$, in which the same moles of HO_2^- generated in the carbon-PTFE cathode are oxidized at the nickel anode. In these conditions, all oxygen consumed at the cathode of the cell is anodically produced and hence, the extraction of oxygen from air occurs by a two-electron process involving Reactions 3 and 5. Energy consumptions between $1.710\,\mathrm{kW\,h\,kg^{-1}}$ O_2 and $1.224\,\mathrm{kW\,h\,kg^{-1}}$ O_2 were obtained at $100\,\mathrm{mA\,cm^{-2}}$, which are significantly lower than those previously reported for other electrochemical oxygen generators.

The two-electron process which takes place in stable Ni–CP cells with $KOH + HO_2^-$ solutions seems more adequate to be applied for the electrochemical production of oxygen from air than previous procedures based on the four-electron anodic oxidation of OH^-. This novel method provides better energy consumptions and can be applied to similar cells containing the carbon–PTFE cathode and other anodes with ability to electrocatalyse the bielectronic anodic oxidation of HO_2^-. Experiments attempting to improve the efficiency of this kind of electrochemical oxygen generator are now in progress in our laboratory.

Acknowledgements

Financial support for this project was provided by Carburos Metálicos S.A. We would like to thank Juan Llibre for his helpful suggestions and Teresa Casado for her help with the English translation.

References

[1] S. H. Langer and R. G. Haldeman, *J. Phys. Chem.* **68** (1964) 962.

[2] A. C. C. Tseung and S. M. Jasem, *J. Appl. Electrochem.* **11** (1981) 209; *US Patent 4 300 987* (1981).

[3] R. A. Wynveen and K. M. Montgomery, *J. Electrochem. Soc.* **114** (1967) 589.

[4] J. R. Goldstein and A. C. C. Tseung, *J. Phys. Chem.* **76** (1972) 3646.

[5] J. Winnick, 'Electrochemical separation of gases', *in* 'Advances in Electrochemical Science and Engineering' (edited by H. Gerischer and C. W. Tobias), vol. 1, VCH, New York (1990), pp. 210–18.

[6] M. Sudoh, T. Kodera, K. Sakai, J. Q. Zhang and K. Koide, *J. Chem. Eng. Japan* **19** (1986) 513.

[7] I. Mathur, A. James and D. Bisset, *US Patent 4 927 509* (1990).

[8] E. Kalu and C. Oloman, *J. Appl. Electrochem.* **20** (1990) 932.

[9] K. Otsuka and I. Yamanaka, *Electrochim. Acta* **35** (1990) 319.

[10] J. S. Do and C. P. Chen, *J. Electrochem. Soc.* **140** (1993) 1632.

[11] P. Tatapudi and J. M. Fenton, *ibid.* **140** (1993) L55.

[12] Y. L. Hsiao and K. Nobe, *J. Appl. Electrochem.* **23** (1993) 943.

[13] E. Brillas, R. M. Bastida, E. LLosa and J. Casado, *J. Electrochem. Soc.* **142** (1995) 1733.

[14] E. Yeager, *Electrochim. Acta* **29** (1984) 1572.

[15] P. Fischer and J. Heitbaum, *J. Electroanal. Chem.* **112** (1980) 231.

[16] Y. Shimizu, K. Uemura, H. Matsuda, N. Miura and N. Yamazoe, *J. Electrochem. Soc.* **137** (1990) 3430.